ACS OMEGA

http://pubs.acs.org/journal/acsodf

Article

External Electric Field-Induced the Modulation of the Band Gap and Quantum Capacitance of F-Functionalized Two-Dimensional Sc_2C

She-Hui Yin,* Xiao-Hong Li, Rui-Zhou Zhang, and Hong-Ling Cui

Cite This: *ACS Omega* 2023, 8, 28608−28614

Read Online

ACCESS | Metrics & More | Article Recommendations | Supporting Information

ABSTRACT: The modulation of electronic properties and quantum capacitance of Sc_2CF_2 under a perpendicular external E-field was investigated using density functional calculations for the potential application of nanoelectronics and nanophotonics. Sc_2CF_2 has an indirect band gap of 0.959 eV without an E-field. Furthermore, it undergoes a semiconducting-metallic transition under a positive E-field and a semiconductor−insulator transition under a negative E-field. The application of the negative E-field makes Sc_2CF_2 have an indirect band gap. Sc-d, F-p, and C-p states are mainly responsible for the significant variation of the band gap. Sc_2CF_2 under an external E-field always keeps the character of a cathode material under the whole potential. Especially, Sc_2CF_2 under a negative external E-field is more suitable for the cathode material due to its much smaller $|Q_p|/|Q_n|$ with much higher Q_n. The charge analysis is further performed.

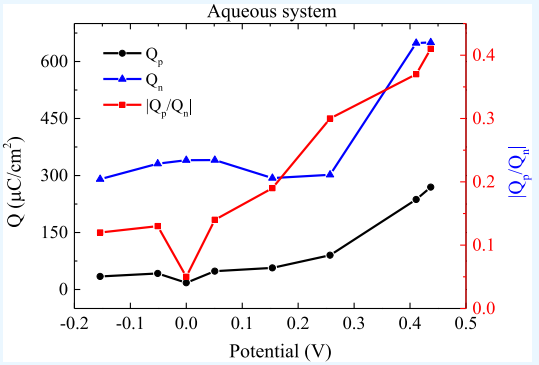

1. INTRODUCTION

Two-dimensional (2D) materials have become the main research field because of their superior electronic properties,[1−3] which boost their applications widely in optoelectronics.[4−6] The zero-band gap for graphene[7] hampers its application in electronic components. Therefore, finding potential materials with a moderate band gap is an effective method to widen their practical applications.

Supercapacitors are one of the most potential energy sources with long cyclic lift and good stability but low energy density.[8,9] Layered 2D materials have superior electrochemical and optoelectronic performance[10−12] and are often used as electrode materials. Research indicates that novel electrode materials with high capacitance can increase the energy density[13] and have higher capacitance, better conductivity, etc.[14] Graphene has a theoretical specific area of 2630 m^2/g,[15] but its capacitance performance should be enhanced.[16−18] Quantum capacitance (C_{diff}) can greatly improve the total capacitance of materials and is determined by the electronic structures of materials.[19] Therefore, developing novel 2D materials to improve C_{diff} is one of the hot topics to enhance the capacitance performance of supercapacitors.

Recently, a new family of 2D materials, MXenes, with the formula of $M_{n+1}X_nT_x$ (M is Ti, Hf, Sc, etc., X is a C or N atom, and T is the termination group such as F, O, and OH), are prepared by etching A layers from MAX phases.[20,21] MXene-based electrode materials are investigated because of their superior characteristics, such as good electrical conductivity.[22,23] Most MXenes are generally metallic, but Sc_2CF_2 is a semiconductor, which can be used in nanoelectronics.[24−26] An external electric field (EEF)[27] or strain[28] can engineer the band gap of a system to meet the requirements in the fields of semiconducting and optics.

An EEF is often utilized to change the electronic properties of 2D materials because of its precise control,[29−32] thus modulating the quantum capacitance. The band gap of MoS_2 under an EEF is engineered,[33] and a vertical EEF can greatly modulate the band gap of MoS_2. The modulation of the band gap in bilayer transition-metal dichalcogenides by the EEF is investigated, and the band gap of the system decreases with increasing EEF, which is related to the Stark effect.[32] Li et al.[34] investigated the band gap of the Sc_2CO_2 bilayer under an EEF. Previous research studies show that the EEF has little effect on some pristine monolayer materials like graphene and silicene.[35−37] However, considerable band gap transition was introduced for single-layer GaN under an EEF.[38] So, we think that an EEF can also affect the other functionalized monolayers.

MXenes are always terminated with surface groups such as F, OH, and O groups, depending on etching agents and subsequent treatment. During etching, the often-used etching agent is hydrofluoric acid (HF); therefore, the higher concentration of −F groups on the surface of MXene is found experimentally.[39,40] For this reason, we chose Sc_2CF_2

Received: May 5, 2023
Accepted: July 17, 2023
Published: July 26, 2023

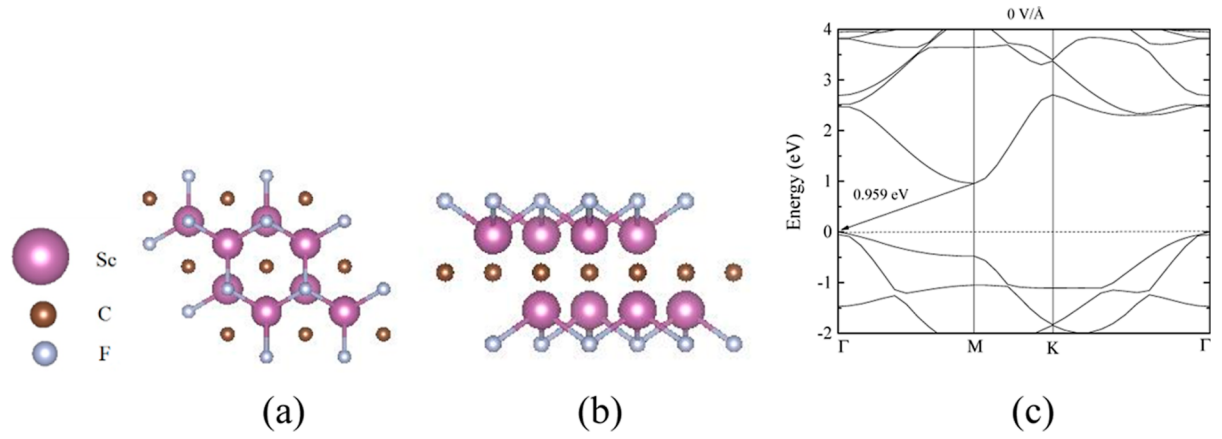

Figure 1. Atomic structure as ball-and-stick models. (a) Sc_2CF_2 monolayer top view; (b) Sc_2CF_2 monolayer side view; (c) band structure of the Sc_2CF_2 monolayer without an EEF. Bouquet, copper, and light-gray colors represent Sc, C, and F atoms, respectively.

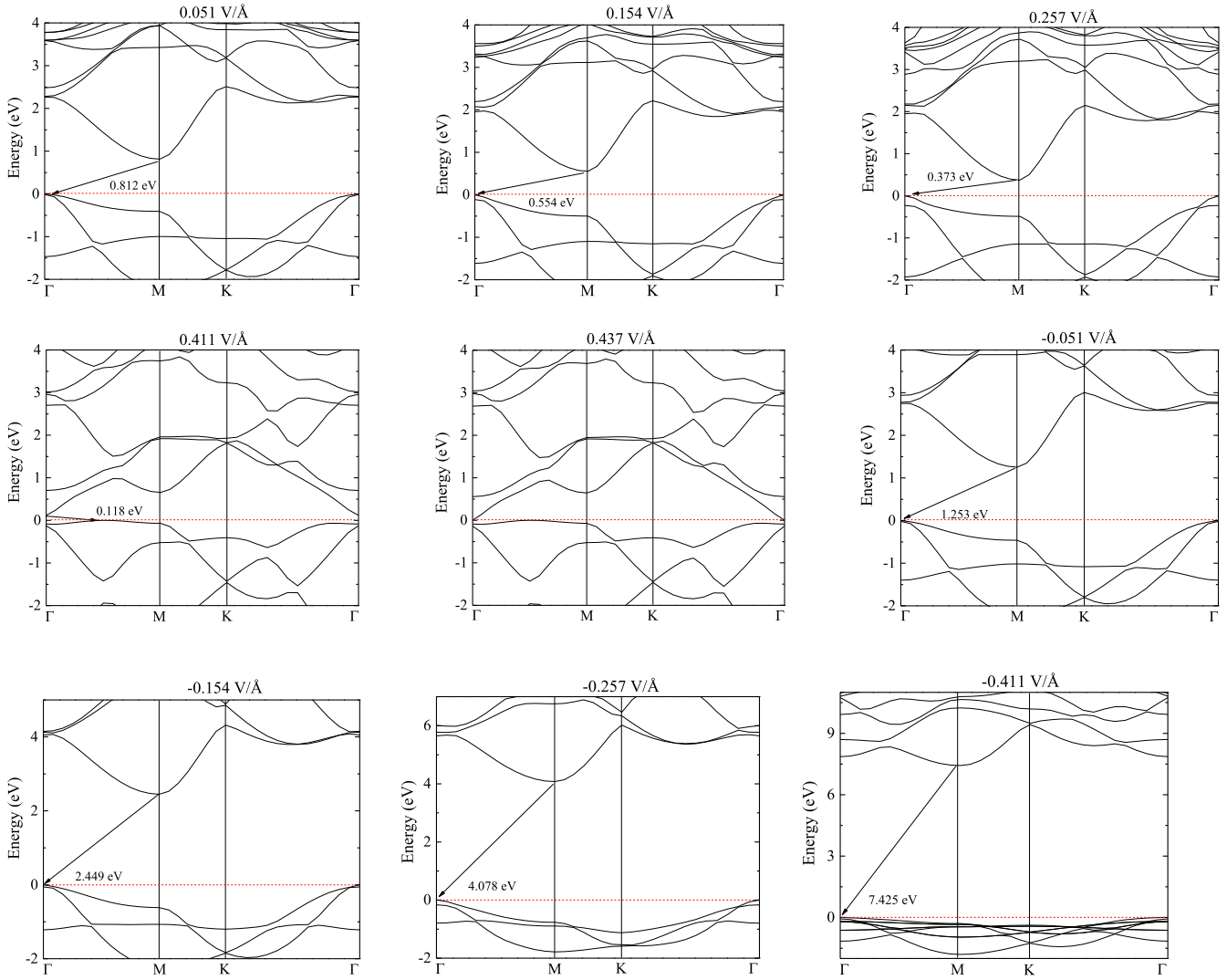

Figure 2. Band structure of the Sc_2CF_2 monolayer.

MXene to investigate its related properties. Pure Sc_2C is a metal, and Sc_2CF_2 has a semiconducting character. The band gap of Sc_2CF_2 monolayer obviates the need for band gap engineering in nanoelectronics and nanophotonics.[41] The engineering of the band gap for the Sc_2CF_2 monolayer is important to widen the applications in the fields of semiconducting and optics.

We herein investigated the electronic properties and C_{diff} of the Sc_2CF_2 monolayer under an EEF normal to the monolayer. The Sc_2CF_2 monolayer under an EEF undergoes the semiconductor−metal transition at about 0.437 V/Å and the

https://doi.org/10.1021/acsomega.3c03102
ACS Omega 2023, 8, 28608−28614

semiconductor−insulator transition at about −0.257 V/Å. The relationship between the band gap and the external field is also presented, which we hope experimental scientists will test.

2. COMPUTATIONAL DETAILS

All calculations were performed by the Dmol^3 code.[42] The GGA-PBE functional[43,44] was used. Double numerical plus polarization was utilized and exhibited better accuracy.[45] A 25 Å vacuum layer was established to eliminate any unnecessary interaction between layers. 15 × 15 × 1 and 31 × 31 × 1 k-mesh were used for optimization and density of state (DOS). All atoms were fully optimized. The convergence in energy and force is 1×10^{-5} Ha and 0.002 Ha/Å, respectively. The calculation of the EEF is performed by adding an artificial dipole to the vacuum level.[46] The EEF is in the direction normal to the Sc_2CF_2 monolayer with a range from −0.411 to +0.436 V/Å.

3. RESULTS AND DISCUSSION

3.1. Structural Properties. Different configurations are considered, and the configuration with F above the Sc atom has the lowest energy, indicating that it has a stable structure. Figure 1a,b presents the structures of the stable Sc_2CF_2 MXene. After the geometry optimization, the lattice constants of a and b without the EEF are 3.2869 and 3.2894 Å, respectively. The electronic band structure (Figure 1c) without the EEF is investigated, and the band gap of the system is 0.959 eV, which is in good agreement with refs 47 and 48.

Cohesive energy (E_{coh}) is often used to elucidate phase stability. For Sc_2CF_2 MXenes, E_{coh} is obtained by the following equation

$$E_{coh} = \frac{E_{tot}(Sc_2CF_2) - 2E_{atm}(Sc) - E_{atm}(C) - 2E_{atm}(F)}{5} \quad (1)$$

where E_{tot} is the total energy of Sc_2CF_2 and E_{atm} are the energies of free atoms Sc, C, and F, respectively. More negative E_{coh} indicates a more stable structure.

The E_{coh} for Sc_2CF_2 without an EEF is −4.59 eV/atom, which indicates the stability of Sc_2CF_2. The E_{coh} of Sc_2C MXenes without an EEF is calculated to be −3.15 eV/atom, indicating that Sc_2CF_2 MXenes are more stable than Sc_2C MXenes.

3.2. Band Gap Engineering under an EEF. The band structures of the Sc_2CF_2 monolayer under an EEF are presented in Figure 2. Sc_2CF_2 under an EEF has no magnetism. An EEF can effectively modify the band structures of Sc_2CF_2. The band gap without the EEF is an indirect gap with the conduction band minimum (CBM) at the M point and the valence band maximum (VBM) at Γ points (Figure 1c). The band gap of Sc_2CF_2 decreases gradually by applying a positive EEF and is driven to zero under 0.437 V/Å, which indicates that the positive EEF can make the system change from semiconductor to metal. The application of the positive EEF makes the CBM shift to Γ point and the VBM shift to the point between Γ and M at 0.411 V/Å.

The reduction of the band gap under a positive EEF is due to charge distribution, which originates in the asymmetry of electronic potential. Under a positive EEF, the conduction band edge moves down because of the electrostatic potential, which gives rise to the reduction of the band gap. The band gap of Sc_2CF_2 increases continuously by applying a negative EEF, and Sc_2CF_2 undergoes the semiconductor−insulator transition, with a band gap of 4.078 eV at −0.257 V/Å and 7.425 eV at −0.411 V/Å. We can note that the band gap increases drastically with the increasing negative EEF and keeps the indirect gap between the M and Γ points.

The energy per atom is investigated to explore the influence of an EEF on electronic properties. The energy under an EEF is $E_{E\text{-field}} = (E_{without\text{-}field} - E_{E\text{-field}})/n$, where n is the atomic number in a unit cell. Figure 3 plots the band gap and energy under an EEF. The character of the quadratic function for the energy under an EEF indicates that the applied EEF is within the limit.

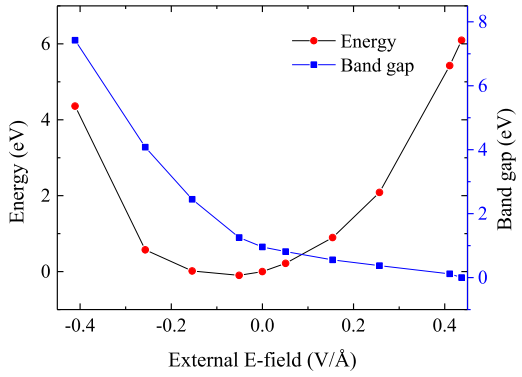

Figure 3. Effect of an EEF on the band gap and energy of Sc_2CF_2 MXene.

From Figure 3, the band gap decreases linearly with the EEF in the range of −0.411 to 0.437 V/Å. The most important finding in this paper is that (1) the band gap increases with the negative EEF and undergoes the semiconductor−insulator transition at about −0.257 V/Å; (2) the band gap reduces with the increasing positive EEF and has the semiconductor−metal transition. It is noted that the band gap under the EEF can be engineered from 0 to 7.425 eV, which indicates that the EEF is an effective strategy to modulate the band gap of Sc_2CF_2.

The partial density of states (PDOS) of the Sc_2CF_2 monolayer is presented in Figure 4. We list the PDOS of Sc_2CF_2 with the EEF of −0.257, 0, and +0.437 V/Å in Figure 4. Sc-d states have strong interactions with C-p states around −1.5 eV and with F-d states around −5.5 eV without the EEF. With the increasing negative EEF, the energy at which Sc-d and F-d states interact shifts toward the right and is about −2.7 eV. The energy at which Sc-d and C-p states interact shifts toward the right with the increasing positive EEF and is −0.5 eV, while the interaction between Sc-d and F-d states disappears at 0.437 V/Å.

C-p states without the EEF have two peaks (labeled in Figure 4) at around −2 eV. With the increase of the negative EEF, the two peaks converge into one peak. From Figure 4, the CBM state without the EEF originates from Sc-d states, while the VBM originates from Sc-d and C-p states. When the EEF is −0.257 V/Å, the VBM state is mainly from Sc-d, F-p, and C-p states, and Sc-d states provide the main contribution of the CBM. With the increasing negative EEF, the energy of the Sc-d state from the CBM state shifts to higher energy gradually, and the band gap increases. The blueshift of Sc-d and C-p states from the VBM state makes Sc_2CF_2 monolayer metalized. DOS around the Fermi level at +0.437 V/Å is mainly from the Sc-d and C-p states.

https://doi.org/10.1021/acsomega.3c03102
ACS Omega 2023, 8, 28608−28614

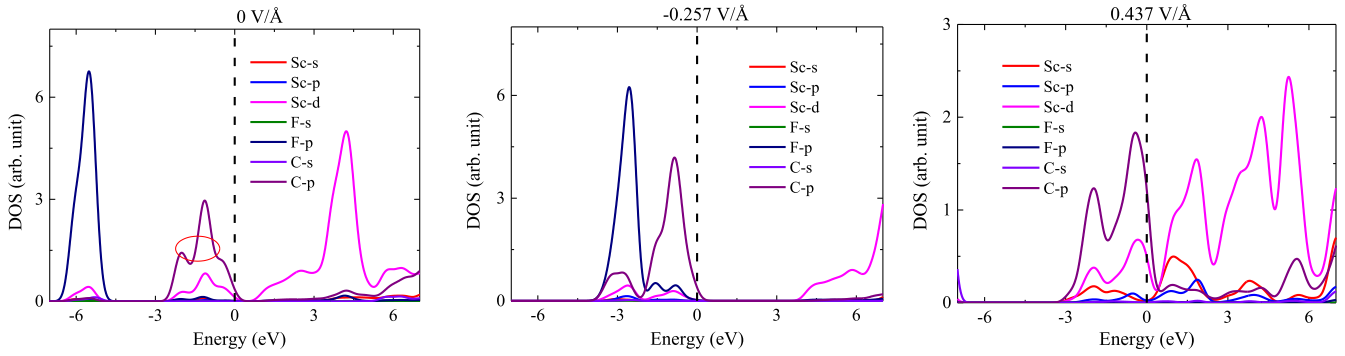

Figure 4. PDOS of Sc_2CF_2 under an EEF.

3.3. Bader Charge under an EEF. Figure 5 presents the Bader charge of Sc, C, and F atoms under an EEF. Sc is the center of the positive charge and donates electrons to C and F atoms, and the negative charge accumulates around C and F atoms. The charges on Sc, C, and F atoms without an EEF are 1.275, −1.363, and −0.594 e−., respectively. With the increasing negative EEF, the charges on the Sc atom decrease gradually, then drastically decrease to 0.732 e− at −0.411 V/Å. Similarly, the charges on C and F atoms increase gradually and then have a drastic increase at −0.411 V/Å. So, there are strong Sc−C and Sc−F interactions in the system. The Sc−F interaction decreases under the EEF of −0.411 V/Å, which is induced by the built-in electric field generated by spontaneous polarization.

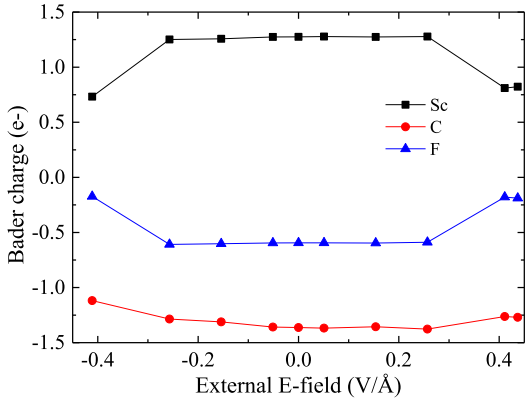

Figure 5. Bader charge of Sc, C, and F atoms under an EEF.

The charges on the Sc atom slightly fluctuate with the increasing positive EEF, then have a drastic decrease when the EEF is larger than 0.411 V/Å. Similarly, the charges on C and F atoms also have a fluctuation, then have a drastic increase. So, the Sc−C and Sc−F interactions decrease above the EEF of 0.411 V/Å.

3.4. Quantum Capacitance of Sc_2CF_2 under an EEF. Quantum capacitance of 2D materials is calculated according to ref 49. Figure 6 presents the total DOS, C_{diff}, and surface storage charge (Q) in the potential range of ±0.6 V (for aqueous electrolytes) and ±1.2 V (for ionic/organic electrolytes). Considering the insulator character of the system with a larger band gap of 4.078 eV at −0.257 V/Å, we only consider the C_{diff} and Q with the EEF from −0.154 to 0.437 V/Å.

From Figure 6a,c, at 0 V, the C_{diff} of Sc_2CF_2 under a positive EEF are generally larger than those under a negative EEF. The C_{diff} of Sc_2CF_2 at 0 V is 170.08 $\mu F/cm^2$. The C_{diff} of Sc_2CF_2 under −0.051 and −0.154 V/Å are 242.10 and 197.39 $\mu F/cm^2$, respectively. The C_{diff} of Sc_2CF_2 are 257.58, 191.80, 210.72, 783.83, and 793.60 $\mu F/cm^2$ for 0.051, 0.154, 0.257, 0.411, and 0.437 V/Å, respectively.

In an aqueous system, the top C_{diff} and Q of Sc_2CF_2 without the EEF at negative and positive potentials are 838.95 $\mu F/cm^2$ and −340.44 $\mu C/cm^2$, 116.59 $\mu F/cm^2$ and 17.61 $\mu C/cm^2$, respectively. Under a negative EEF, the C_{diff} of Sc_2CF_2 at positive potential tends to be zero, and their top C_{diff} and Q at negative potential are 786.70, 791.85, $\mu F/cm^2$, and −331.13, −290.44 $\mu C/cm^2$ for −0.051, −0.154 V/Å, respectively. The top Q at positive potential (CBE_p) are 42.32 and 34.30 $\mu C/cm^2$ for −0.051 and −0.154 V/Å, respectively. Under a positive EEF, the top C_{diff} at a negative potential (C_n) fluctuates with the increasing potential and drastically increases to 1200.57 and 1204.33 $\mu F/cm^2$ at 0.411 and 0.437 V/Å, respectively. Similarly, their top C_{diff} at positive potential (C_p) also has a drastic increase at 0.411 and 0.437 V/Å, with 701.90 and 715.86 $\mu F/cm^2$, respectively. The Q_p increases with the increasing potential, while the top Q at a negative potential (Q_n) fluctuates and increases to −648.58 and −650.15 $\mu C/cm^2$ at 0.411 and 0.437 V/Å, respectively. In an ionic/organic system, the wide potential generally greatly improves the C_n and Q_n.

The ratio of Q_p and Q_n is used to predict the preferred electrode type. Figure 7 shows the Q_p, Q_n, and $|Q_p|/|Q_n|$ in whole potential. $|Q_p|/|Q_n|$ in the aqueous system for Sc_2CF_2 under an EEF are all smaller than 1, indicating that Sc_2CF_2 under the EEF is suitable as cathode material. Especially, the system without the EEF has more potential as a cathode material due to the lower $|Q_p|/|Q_n|$ with higher Q_n and lower Q_p. Sc_2CF_2 under an EEF keeps the character of the cathode material under wide potential. We can note that Sc_2CF_2 under a negative EEF is more suitable for the cathode material due to its much smaller $|Q_p|/|Q_n|$ with much higher Q_n. Table S1 lists the Q_p, Q_n, $|Q_p|/|Q_n|$, and the electrode type in the whole potential.

4. CONCLUSIONS

In this paper, the modulation of electronic structures and quantum capacitance of monolayer Sc_2CF_2 under an EEF is theoretically investigated. Our investigation indicates that the EEF is an effective method to engineer the band gap of Sc_2CF_2. Sc_2CF_2 changes from semiconductor to conductor with the increasing positive EEF. With the increasing negative EEF, Sc_2CF_2 undergoes the semiconductor−insulator transition at −0.257 V/Å. The band gap is 7.425 eV at about −0.411 V/Å. The blue shift of Sc-d and C-p states from the VBM state

https://doi.org/10.1021/acsomega.3c03102
ACS Omega 2023, 8, 28608−28614

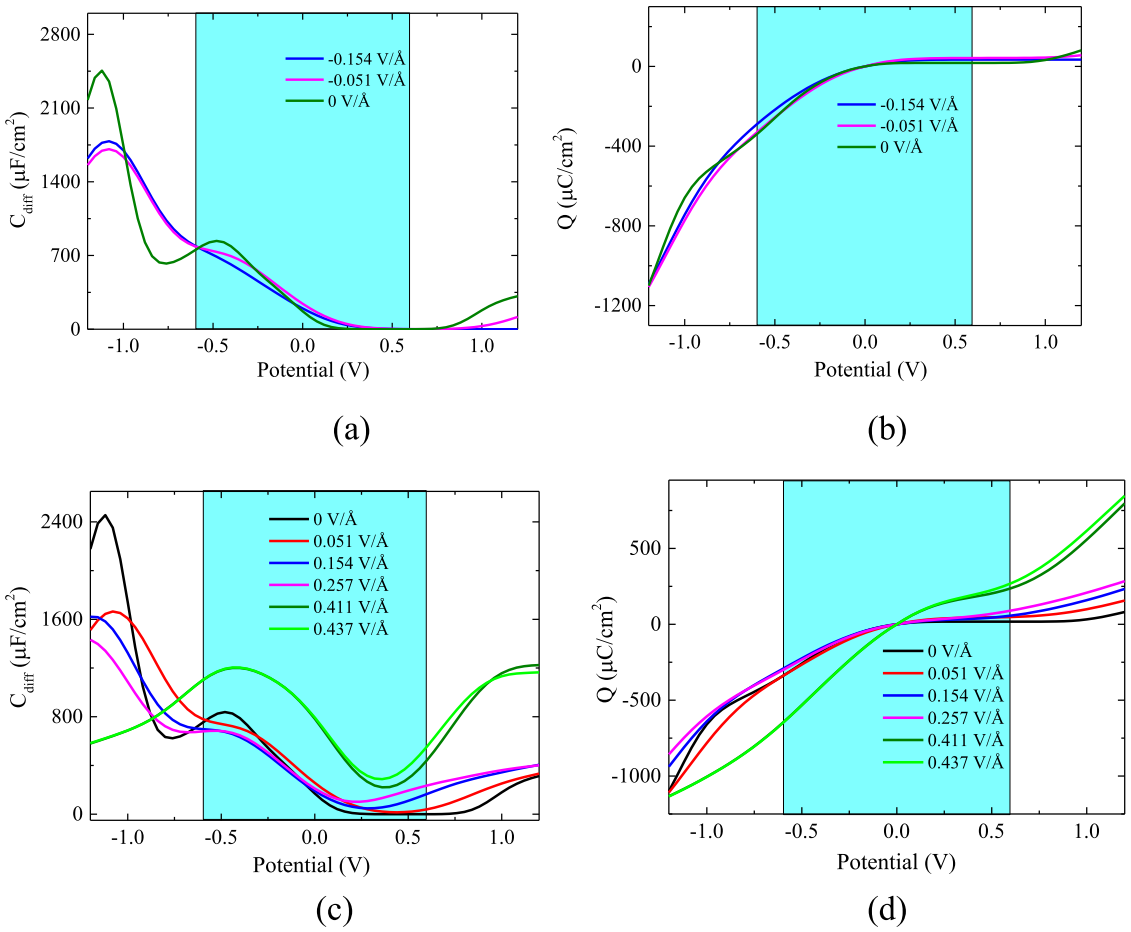

Figure 6. Quantum capacitance (a,c) and surface storage charge (b,d) of Sc_2CF_2 under an EEF.

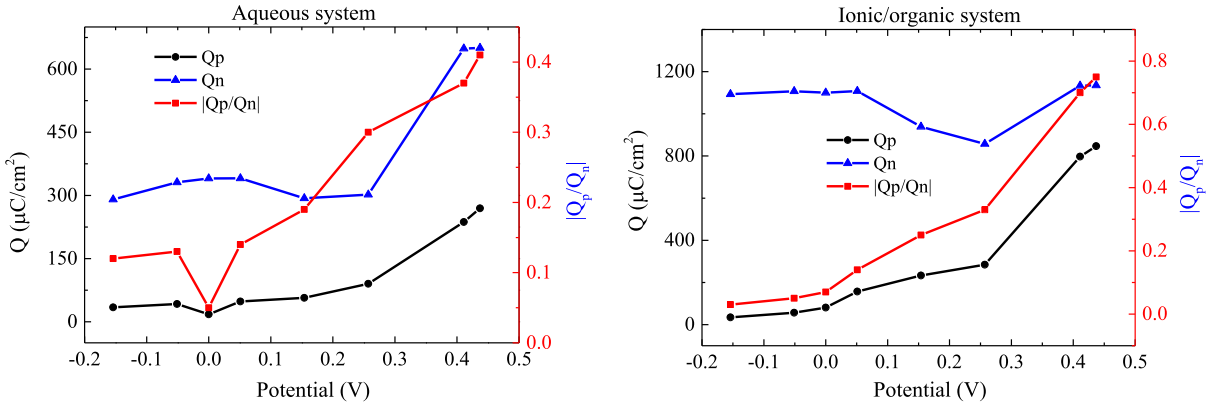

Figure 7. Q_p, Q_n, and $|Q_p|/|Q_n|$ in aqueous and ionic/organic systems.

induces the metallization of Sc_2CF_2 with increasing positive EEF. With the increasing negative EEF, the blueshift of Sc-d states from the CBM state induces the increase of band gap. Sc−C and Sc−F interactions decrease with the increasing positive EEF. Sc_2CF_2 under an EEF is a potential cathode material under the whole potential, and the wide potential greatly improves the C_n and Q_n.

■ ASSOCIATED CONTENT

Supporting Information

The Supporting Information is available free of charge at https://pubs.acs.org/doi/10.1021/acsomega.3c03102.

Q_p, Q_n, $|Q_p|/|Q_n|$, and the electrode type in whole potential (PDF)

■ AUTHOR INFORMATION

Corresponding Author

She-Hui Yin − *Physical Teaching and Research of Fundamental Teaching Section, Henan Polytechnic Institute, Nanyang 473000, China*; Email: 15936166712@163.com

https://doi.org/10.1021/acsomega.3c03102
ACS Omega 2023, 8, 28608−28614

Authors

Xiao-Hong Li − *College of Physics and Engineering, Henan University of Science and Technology, Luoyang 471023, China;* orcid.org/0000-0003-2450-4476

Rui-Zhou Zhang − *College of Physics and Engineering, Henan University of Science and Technology, Luoyang 471023, China*

Hong-Ling Cui − *College of Physics and Engineering, Henan University of Science and Technology, Luoyang 471023, China*

Complete contact information is available at: https://pubs.acs.org/10.1021/acsomega.3c03102

Notes

The authors declare no competing financial interest.

■ ACKNOWLEDGMENTS

The authors acknowledge the Key Scientific and Technological Projects in Henan Province (232102220023).

■ REFERENCES

(1) Geim, A. K. Graphene: Status and Prospects. *Science* **2009**, *324*, 1530−1534.

(2) Tang, Q.; Zhou, Z. Graphene-analogous low-dimensional materials. *Prog. Mater. Sci.* **2013**, *58*, 1244−1315.

(3) Zhang, X.; Xie, Y. Recent advances in free-standing two-dimensional crystals with atomic thickness: design, assembly, and transfer strategies. *Chem. Soc. Rev.* **2013**, *42*, 8187−8199.

(4) Dean, C. R.; Young, A. F.; Meric, I.; Lee, C.; Wang, L.; Sorgenfrei, S.; Watanabe, K.; Taniguchi, T.; Kim, P.; Shepard, K. L.; Hone, J. Boron Nitride substrates for high-quality graphene electronics. *Nat. Nanotechnol.* **2010**, *5*, 722−726.

(5) Molle, A.; Goldberger, J.; Houssa, M.; Xu, Y.; Zhang, S. C.; Akinwande, D. Buckled two-dimensional Xene sheets. *Nature materials* **2017**, *16*, 163−169.

(6) Meng, R.; da Costa Pereira, L.; Locquet, J. P.; Afanas'ev, V.; Pourtois, G.; Houssa, M. Hole-doping induced ferromagnetism in 2D materials. *npj Comput. Mater.* **2022**, *8*, 230.

(7) Novoselov, K. S.; Jiang, D.; Schedin, F.; Booth, T. J.; Khotkevich, V. V.; Morozov, S. V.; Geim, A. K. Two- dimensional atomic crystals. *Proc. Natl. Acad. Sci. U.S.A.* **2005**, *102*, 10451−10453.

(8) Sikdar, A.; Majumdar, A.; Dutta, P.; Borah, M.; Kim, S. O.; Maiti, U. N. Ultra-large area graphene hybrid hydrogel for customized performance supercapacitors: high volumetric, areal energy density and potential wearability. *Electrochim. Acta* **2020**, *332*, 135492.

(9) Chen, T.; Li, S.; Ma, L.; Zhao, X.; Fang, G. Aldehyde reduced Co_3O_4 to form oxygen vacancy and enhance the electrochemical performance for oxygen evolution reaction and supercapacitors. *Nanotechnology* **2019**, *30*, 395403.

(10) Gutiérrez, H. R. Two-dimensional layered materials offering expanded applications in Flatland. *ACS Appl. Nano Mater.* **2020**, *3*, 6134−6139.

(11) Zhan, H.; Guo, D.; Xie, G. Two-dimensional layered materials from mechanical and coupling properties towards applications in electronics. *Nanoscale* **2019**, *11*, 13181−13212.

(12) Zhou, Y.; Zhai, G.; Yan, T.; Huang, Q.; Guo, Z.; Lin, C. T.; Du, S. Current rectification induced by V-doped and Sc-doped in Ti_2CO_2 devices. *Comput. Mater. Sci.* **2017**, *138*, 175−182.

(13) Yang, J.; Li, P. F.; Wang, L. J.; Guo, X. W.; Guo, J.; Liu, S. In-situ synthesis of Ni−MOF@CNT on graphene/Ni foam substrate as a novel self-supporting hybrid structure for all-solid-state supercapacitors with a high energy density. *J. Electroanal. Chem.* **2019**, *848*, 113301.

(14) Hu, R. M.; Shang, J. X. Quantum capacitance of transition metal and nitrogen co−doped graphenes as supercapacitors electrodes: A DFT study. *Appl. Surf. Sci.* **2019**, *496*, 143659.

(15) Yang, G. M.; Zhang, H. Z.; Fan, X. F.; Zheng, W. T. Density functional theory calculations for the quantum capacitance performance of graphene-based electrode material. *J. Phys. Chem. C* **2015**, *119*, 6464−6470.

(16) Zhao, J. W.; Chen, J.; Xu, S. M.; Shao, M. F.; Zhang, Q.; Wei, F.; Ma, J.; Wei, M.; Evans, D. G.; Duan, X. Hierarchical NiMn layered double hydroxide/carbon nanotubes architecture with superb energy density for flexible supercapacitors. *Adv. Funct. Mater.* **2014**, *24*, 2938−2946.

(17) Zhou, X.; Shen, X.; Xia, Z.; Zhang, Z.; Li, J.; Ma, Y.; Qu, Y. Hollow fluffy Co_3O_4 cages as efficient electroactive materials for supercapacitors and oxygen evolution reaction. *ACS Appl. Mater. Interfaces* **2015**, *7*, 20322−20331.

(18) Hung, T. F.; Yin, Z. W.; Betzler, S. B.; Zheng, W. J.; Yang, J.; Zheng, H. M. Nickel sulfide nanostructures prepared by laser irradiation for efficient electrocatalytic hydrogen evolution reaction and supercapacitors. *Chem. Eng. J.* **2019**, *367*, 115−122.

(19) Paek, E.; Pak, A. J.; Hwang, G. S. A computational study of the interfacial structure and capacitance of graphene in [BMIM] [PF6] ionic liquid. *J. Electrochem. Soc.* **2013**, *160*, A1−A10.

(20) Li, X. H.; Chagas da Silva, M.; Salahub, D. R. First-principles calculations of the structural, mechanical, electronic and bonding properties of $(CrB_2)_nCrAl$ with n = 1, 2, 3, J. Alloy. *Compds* **2017**, *698*, 291−303.

(21) Dahlqvist, M.; Alling, B.; Rosen, J. Stability trends of MAX phases from first principles. *Phys. Rev. B: Condens. Matter Mater. Phys.* **2010**, *81*, 220102.

(22) Zhang, X.; Zhang, Z.; Zhou, Z. MXene-based materials for electrochemical energy storage. *J. Energy Chem.* **2018**, *27*, 73−85.

(23) Xiong, D.; Li, X.; Bai, Z.; Lu, S. Recent Advances in Layered $Ti_3C_2T_x$ MXene for Electrochemical Energy Storage. *Small* **2018**, *14*, 1703419.

(24) Ayari, A.; Cobas, E.; Ogundadegbe, O.; Fuhrer, M. S. Realization and electrical characterization of ultrathin crystals of layered transition- metal dichalcogenides. *J. Appl. Phys.* **2007**, *101*, 014507.

(25) Mak, K.; Lee, C.; Hone, J.; Shan, J.; Heinz, T. Atomically thin MoS_2: A new direct-gap semiconductor. *Phys. Rev. Lett.* **2010**, *105*, 136805.

(26) Radisavljevic, B.; Radenovic, A.; Brivio, J.; Giacometti, V.; Kis, A. Single-layer MoS_2 transistors. *Nat. Nanotechnol.* **2011**, *6*, 147−150.

(27) Lee, Y.; Hwang, Y.; Cho, S. B.; Chung, Y.-C. Achieving a direct band gap in oxygen functionalized-monolayer scandium carbide by applying an electric field. *Phys. Chem. Chem. Phys.* **2014**, *16*, 26273−26278.

(28) Lee, Y.; Cho, S. B.; Chung, Y.-C. Tunable Indirect to Direct Band Gap Transition of Monolayer Sc2CO2 by the Strain Effect. *ACS Appl. Mater. Interfaces* **2014**, *6*, 14724−14728.

(29) Castro, E. V.; Novoselov, K.; Morozov, S.; Peres, N.; dos Santos, J. M. B. L.; Nilsson, J.; Guinea, F.; Geim, A.; Neto, A. H. C. Biased bilayer graphene: semiconductor with a gap tunable by the electric field effect. *Phys. Rev. Lett.* **2007**, *99*, 216802.

(30) Samarakoon, D. K.; Wang, X. Q. Tunable band gap in hydrogenated bilayer graphene. *ACS Nano* **2010**, *4*, 4126−4130.

(31) Ramasubramaniam, A.; Naveh, D.; Towe, E. Tunable band gaps in bilayer graphene-BN heterostructures. *Nano Lett.* **2011**, *11*, 1070−1075.

(32) Ramasubramaniam, A.; Naveh, D.; Towe, E. Tunable band gaps in bilayer transition-metal dichalcogenides. *Phys. Rev. B: Condens. Matter Mater. Phys.* **2011**, *84*, 205325−205335.

(33) Qi, J.; Li, X.; Qian, X.; Feng, J. Bandgap engineering of rippled MoS_2 monolayer under external electric field. *Appl. Phys. Lett.* **2013**, *102*, 173112.

(34) Li, L. Effects of the interlayer interaction and electric field on the band gap of polar bilayers: a case study of Sc_2CO_2. *J. Phys. Chem. C* **2016**, *120*, 24857−24865.

(35) Xu, D.; He, H.; Pandey, R.; Karna, S. P. Stacking and electric field effects in atomically thin layers of GaN. *J. Phys.: Condens. Matter* **2013**, *25*, 345302.

(36) Ni, Z.; Liu, Q.; Tang, K.; Zheng, J.; Zhou, J.; Qin, R.; Gao, Z.; Yu, D.; Lu, J. Tunable bandgap in silicene and germanene. *Nano Lett.* **2011**, *12*, 113−118.
(37) Drummond, N.; Zolyomi, V.; Fal'Ko, V. Electrically tunable band gap in silicene. *Phys. Rev. B: Condens. Matter Mater. Phys.* **2012**, *85*, 075423.
(38) Chen, Q.; Hu, H.; Chen, X.; Wang, J. Tailoring band gap in GaN sheet by chemical modification and electric field: Ab initio calculations. *Appl. Phys. Lett.* **2011**, *98*, 053102.
(39) Naguib, M.; Halim, J.; Lu, J.; Cook, K. M.; Hultman, L.; Gogotsi, Y.; Barsoum, M. W. New two-dimensional niobium and vanadium carbides as promising materials for li-ion batteries. *J. Am. Chem. Soc.* **2013**, *135*, 15966−15969.
(40) Harris, K. J.; Bugnet, M.; Naguib, M.; Barsoum, M. W.; Goward, G. R. Direct measurement of surface termination groups and their connectivity in the 2D MXene V2CT*x* using NMR spectroscopy. *J. Phys. Chem. C* **2015**, *119*, 13713−13720.
(41) Khazaei, M.; Arai, M.; Sasaki, T.; Chung, C.-Y.; Venkataramanan, N. S.; Estili, M.; Sakka, Y.; Kawazoe, Y. Novel electronic and magnetic properties of two-dimensional transition metal carbides and nitrides. *Adv. Funct. Mater.* **2013**, *23*, 2185−2192.
(42) Delley, B. From molecules to solids with the DMol3 approach. *J. Chem. Phys.* **2000**, *113*, 7756−7764.
(43) Perdew, J. P.; Burke, K.; Ernzerhof, M. Generalized gradient approximation made simple. *Phys. Rev. Lett.* **1996**, *77*, 3865−3868.
(44) Wang, Y.; Perdew, J. P. Correlation hole of the spin-polarized electron gas, with exact small-wave-vector and high-density scaling. *Phys. Rev. B: Condens. Matter Mater. Phys.* **1991**, *44*, 13298−13307.
(45) Wang, M.; Liu, H.; Huang, Z.-H.; Kang, F. Activated carbon fibers loaded with MnO2 for removing NO at room temperature. *Chem. Eng. J.* **2014**, *256*, 101−106.
(46) Neugebauer, J.; Scheffler, M. Adsorbate-substrate and adsorbate-adsorbate interactions of Na and K adlayers on Al(111). *Phys. Rev. B: Condens. Matter Mater. Phys.* **1992**, *46*, 16067−16080.
(47) Balcı, E.; Akkuş, Ü. Ö.; Berber, S. Band gap modification in doped MXene: Sc_2CF_2. *J. Mater. Chem. C* **2017**, *5*, 5956−5961.
(48) Yang, J.; Luo, X.; Zhang, S.; Chen, L. Investigation of magnetic and electronic properties of transition metal doped Sc_2CF_2 (T=O, OH, or F) using a first principles study. *Phys. Chem. Chem. Phys.* **2016**, *18*, 12914−12919.
(49) Xu, Q.; Yang, G. M.; Fan, X. F.; Zheng, W. T. Improving the quantum capacitance of graphene-based supercapacitors by the doping and co-doping: First-principles calculations. *ACS. Omega.* **2019**, *4*, 13209−13217.

https://doi.org/10.1021/acsomega.3c03102
ACS Omega 2023, 8, 28608−28614